Available online at www.sciencedirect.com
SCIENCE DIRECT®
Composites Science and Technology 63 (2003) 1637–1646
COMPOSITES SCIENCE AND TECHNOLOGY
www.elsevier.com/locate/compscitech

Electrical properties of single wall carbon nanotube reinforced polyimide composites

Z. Ounaies[a,*], C. Park[b], K.E. Wise[b], E.J. Siochi[c], J.S. Harrison[c]

[a]Department of Mechanical Engineering, Virginia Commonwealth University, Richmond, VA 23284, USA
[b]ICASE, NASA Langley Research Center, MS 132C, Hampton, VA 23681, USA
[c]NASA Langley Research Center, MS 226, Hampton, VA 23681, USA

Received 27 November 2002; received in revised form 17 January 2003; accepted 25 January 2003

Abstract

Electrical properties of single wall carbon nanotube (SWNT) reinforced polyimide composites were investigated as a function of SWNT concentration. AC and DC conductivities were measured, and the frequency behavior of the specific admittance was investigated. The experimental conductivity was found to obey a percolation-like power law with a relatively low percolation threshold. The current-voltage measurement results exhibited a non-ohmic behavior, indicating a quantum tunneling conduction mechanism. Analytical modeling and numerical simulation using high aspect ratio, rigid, spherocylinders as models for the SWNT were carried out to aid in understanding these results. The predictions were in good agreement with the experimental results. Published by Elsevier Ltd.

Keywords: A. Nanostructures; A. Polymers; B. Electrical properties; B. Modelling; Single wall carbon nanotube; Composites

1. Introduction

Polyimides are widely used in applications ranging from microelectronics to aerospace. Due to their insulating nature, significant accumulation of electrostatic charge may result on their surface, causing local heating and premature degradation to electronic components or space structures. This work describes a single wall carbon nanotube (SWNT) reinforced polyimide composite with a level of electrical conductivity sufficient to permit electrostatic discharge, as well as mechanical and thermal properties superior to that of the base polymer.

Over the past decade, great strides have been made in exploiting the unique combination of electronic and mechanical properties of carbon nanotubes (CNT) [1,2]. Several publications document the progress made in fabrication and characterization of CNT nanocomposites [3–6]. Unfortunately, it is difficult to draw definite conclusions about electrical conductivity from these published studies because the reported levels of CNT loading required to achieve a percolation concentration (i.e. an appreciable increase in electrical conductivity) vary widely, ranging from less than 1 to over 10%. Two reasons could account for these differences: (1) the CNT bundles are not sufficiently dispersed in the polymer matrix, and (2) experimental difficulties may result in inaccurate detection of the onset of conductivity. Difficulty in obtaining homogeneously dispersed CNT nanocomposites arises from the non-reactive nature of the CNT surface and the unavoidable bundle formation due to van der Waals attraction during synthesis. Most published work have focused on chemical modification of the CNT to improve dispersion through functionalizaton oxidization, melt mixing, and compounding [3–5]. However, successful dispersion remains elusive. The resulting bundling yields a larger effective diameter of the conductive inclusions. As a result, the aspect ratio appears reduced. The outcome is the first case where increased loading levels are required to successfully achieve percolation. In the second case, instrument sensitivity and sample preparation issues may be masking an initial percolation transition at very low loadings.

This paper seeks to address these percolation issues through a combination of experimental and computational methods. Using a method developed in this lab [7], composite films were prepared with a very high degree of CNT dispersion. The electrical properties of these films were then systematically characterized, using both DC and AC specific measurement techniques.

* Corresponding author. Fax: +1-804-827-7030.
E-mail address: zounaies@vcu.edu (Z. Ounaies).

0266-3538/03/$ - see front matter Published by Elsevier Ltd.
doi:10.1016/S0266-3538(03)00067-8

Finally, these results were interpreted using both an analytical percolation theory model and numerical simulations. The experimental and theoretical results corroborate to suggest a percolation transition at extremely low loading levels of CNT.

2. Experimental

2.1. Synthesis and processing

Purified laser ablated single wall carbon nanotubes (SWNT) were obtained from Rice University. An aromatic colorless polyimide, CP2 [8], was selected as a polymer matrix. The SWNT-CP2 composites were prepared by in situ polymerization under sonication. The density of pure CP2 is about 1.4 g/cm^3, and the calculated density of the SWNT have been reported ranging from 1.33 to 1.40 depending on chirality [9]. Considering unavoidable error (5% in SWNT concentration) in preparation of the SWNT-CP2 solutions and the error margin (8% in lattice parameter) in calculation of SWNT, the weight fraction of SWNT was assumed to be the volume fraction without further correction. The diamine and dianhydride used to synthesize the CP2 were 1,3-bis(3-aminophenoxy) benzene (APB) and 2,2-bis(3,4-anhydrodicarboxyphenyl) hexafluoropropane (6FDA), respectively. SWNT dispersed in anhydrous dimethyl formamide (DMF) was used as a solvent for the CP2 poly(amic acid) synthesis. The entire reaction was carried out with stirring, in a nitrogen-purged flask immersed in a 40 kHz ultrasonic bath until the solution viscosity increased and stabilized. Sonication was terminated after 3 h and stirring was continued for several hours to form a SWNT-poly(amic acid) solution. Acetic anhydride and pyridine were used as catalysts to chemically imidize the SWNT- poly(amic acid). The SWNT-polyimide solution was cast onto a glass plate and dried in a dry air-flowing chamber. Subsequently, the dried tack-free film was thermally cured in an air-circulating oven to obtain solvent-free freestanding SWNT-polyimide film. A series of SWNT-CP2 nanocomposite films were prepared with SWNT concentrations ranging from 0.01 to 1.0 vol.%. Glass transition temperatures of the films were determined by differential scanning calorimetry (DSC) using a Shimadzu DSC-50 at a heating rate of 10 °C/min. Optical properties were evaluated with a Perkin Elmer Lambda 900 UV/vis/NIR spectrophotometer. Mechanical properties were measured by a dynamic mechanical thermal analyzer (DMTA, Rheometrics). Thermal stability was investigated by dynamic thermogravimetric analysis (TGA, Seiko) at a heating rate of 2.5 °C/min in air. A summary of these results is included in this paper, and a more detailed analysis appears in previous publications [7,10,11].

2.2. Electrical measurements

DC volume and surface conductivities of the composites were evaluated according to ASTM D257 using a Keithley 8009 resistivity test fixture and a Keithley 6517 electrometer. The composites were 2.54 mm in diameter, and varied in thickness from 20 to 40 μm.

AC conductivity and admittance as a function of frequency were measured using a HP 4284 LCR meter. The nanocomposite can be modeled as a resistor and capacitor in parallel. The *admittance* Y of such a system is defined as:

$$Y = Y' + jY'' = (1/R_p) + j2\pi f C_p \tag{1}$$

where R_p is the resistance of the composite, C_p is the capacitance, and f is the frequency of measurement. The *specific admittance* y is calculated from the modulus of Y ($|Y|$), and is used to compare the frequency behavior of the composites:

$$y = |Y|\left(\frac{t}{A}\right) \tag{2}$$

where t is the thickness of the composite and A is the area of the electrodes. Current-voltage measurements were performed at room temperature under DC field as a function of SWNT concentration. Temperature dependence of the conductivity of the SWNT-CP2 composites was probed under AC field at 20 Hz using a Sun Systems environmental chamber over the temperature range of 25–150 °C.

3. Results

3.1. Synthesis and processing

SWNT-CP2 composites were prepared by in situ polymerization in the presence of sonication. No significant change in the glass transition temperature of the SWNT-CP2 composites was observed, indicating that the polyimide condensation reaction was not adversely affected by the incorporation of SWNT and sonication. Transmission electron micrographs (TEM) revealed that thin SWNT bundles were dispersed uniformly throughout the whole polymer matrix [7,10,11]. The diameter and length of SWNT were approximately 1.4 nm and 3 μm, respectively [11]. The average thickness of the bundles ranged from 2 to 12 nm according to TEM and magnetic force micrographs [10,11]. Significant improvement in mechanical and thermal properties of the SWNT-CP2 composites resulted from the incorporation of SWNT [7]. The storage modulus of the composites increased linearly with increasing SWNT concentration, reaching a 65% improvement at 1.0 vol.%. The temperature at 5 wt.% loss, measured by TGA, showed an increase of 35 °C at 1.0 vol.%. The

optical transparency of the composites remained high at loading levels up to 1.0 vol.% [7]. This combination of structural, thermal, and optical properties makes these composites ideal for space structures applications.

3.2. DC electrical measurements

The DC volume conductivity results are plotted in Fig. 1 as a function of SWNT concentration. The conductivity of the pristine CP2 polyimide was about 6.3×10^{-18} S/cm. A sharp increase of the conductivity value was observed between 0.02 and 0.1 vol.%, where the conductivity changed from 3×10^{-17} to 1.6×10^{-8} S/cm. At loading levels in excess of 0.1 vol.%, the conductivity increased only moderately. At 0.5 vol.%, the conductivity was 3×10^{-7} S/cm, ten orders of magnitude higher than the value at 0.02 vol.%. This behavior is indicative of a percolation transition. Percolation theory predicts that there is a critical concentration or percolation threshold at which a conductive path is formed in the composite causing the material to convert from a capacitor to a conductor. Fig. 1 indicates that the percolation threshold for this material resides between 0.02 and 0.1 vol.%. It is noted that at 0.1 vol.%, the conductivity level exceeded the antistatic criterion of thin films (1×10^{-8} S/cm), which is the targeted application for these composites.

In order to determine the critical volume concentration, the volume conductivity data was fitted to a power law in terms of volume fraction of SWNT. Fig. 2 shows that a good fit was achieved between the experimental data (triangles) and the fit function (straight line), with a correlation factor $R=99.9\%$. The conductivity is linear with $(v-v_c)$ in a logarithmic scale and the relationship is described by the equation below:

$$\sigma = A(v - v_c)^t \tag{3}$$

where σ is the conductivity of the composite, v is the volume fraction of the SWNT in the composite, v_c is the critical volume fraction (volume fraction at percolation), A and t are fitted constants. A best fit to the data resulted in a value for A of 1×10^{-6} S/cm and t of 1.5 when v_c was assumed to be 0.05 vol.% (percolation threshold value). To our knowledge, this value of the percolation threshold is the lowest reported so far for a polymer-SWNT composite. Theoretical predictions of the critical exponent, t, range from 1.6 to 2.0 [12,13] while experimental values between 1.3 and 3.1 have been reported [12]. The critical exponent of the present composite system is in reasonable agreement with both experimental and theoretical predictions. Theoretically, the value of the constant A should approach the conductivity of the SWNT. In the present case, however, A was lower than expected. To address this deviation and further probe the conduction mechanism in the SWNT-CP2 composites, measurements of the current-voltage (I–V) characteristics were made. Results show that at SWNT loadings in excess of 0.1 vol.%, non-linear I–V relationships are observed (Fig. 3). This non-ohmic behavior is most likely due to a tunneling mechanism.

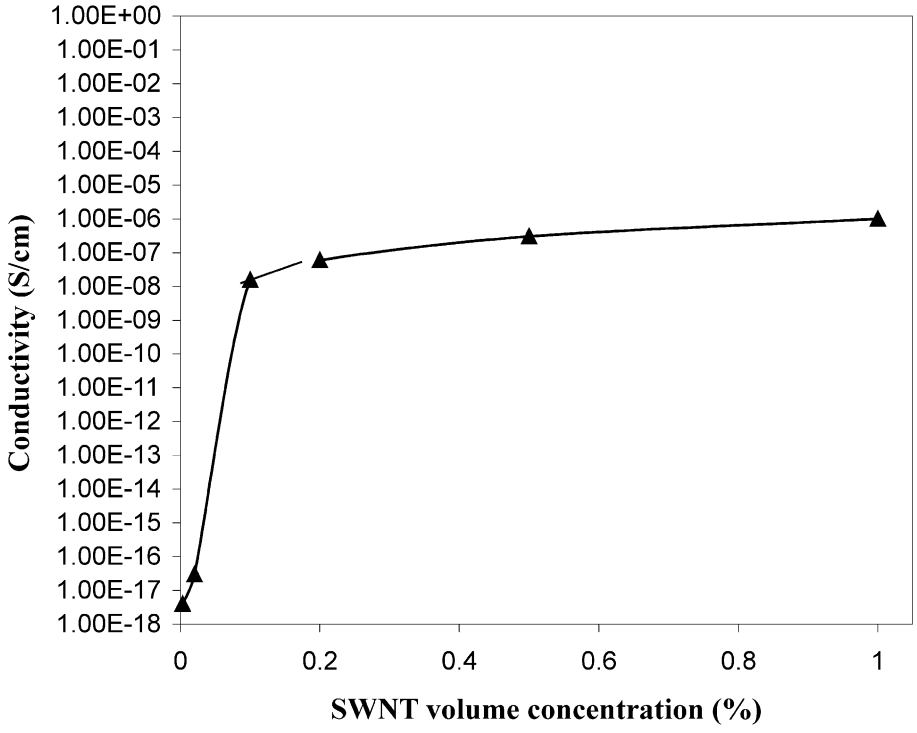

Fig. 1. DC electrical conductivity variations with SWNT volume concentration (1 V).

Conduction may occur by electron hopping from a nanotube to an adjacent one when they are close enough. Above percolation, conductive paths are formed through the composites due to quantum tunneling effects where the distance between the conductive inclusions is such that electron hopping can occur. Percolation theory assumes that paths are made up of conductive inclusions in direct contact. However, in the case of quantum tunneling, a contact resistance exists within the conductive path, in this case between two

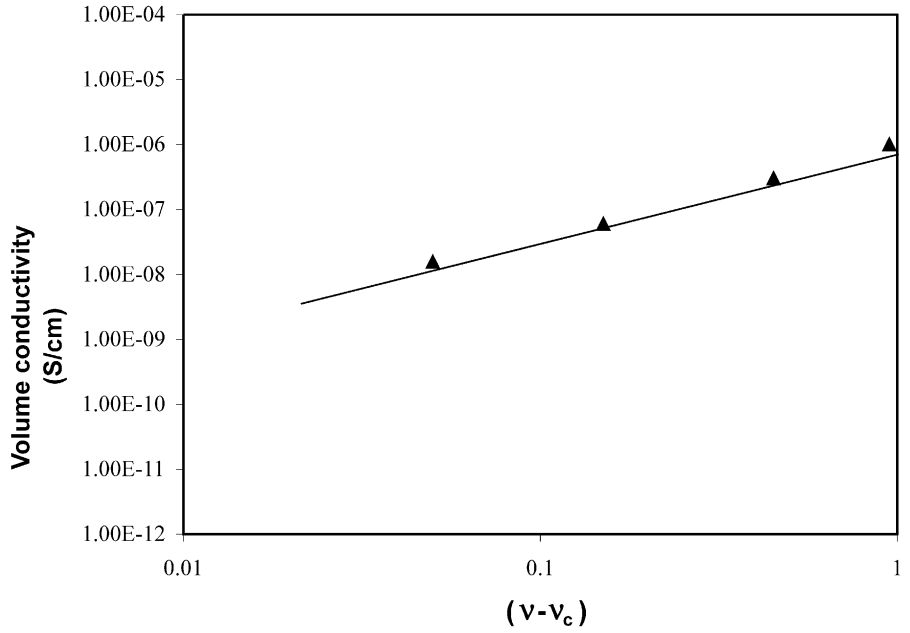

Fig. 2. Percolation equation fit to the experimental data (DC conductivity data from Fig. 1).

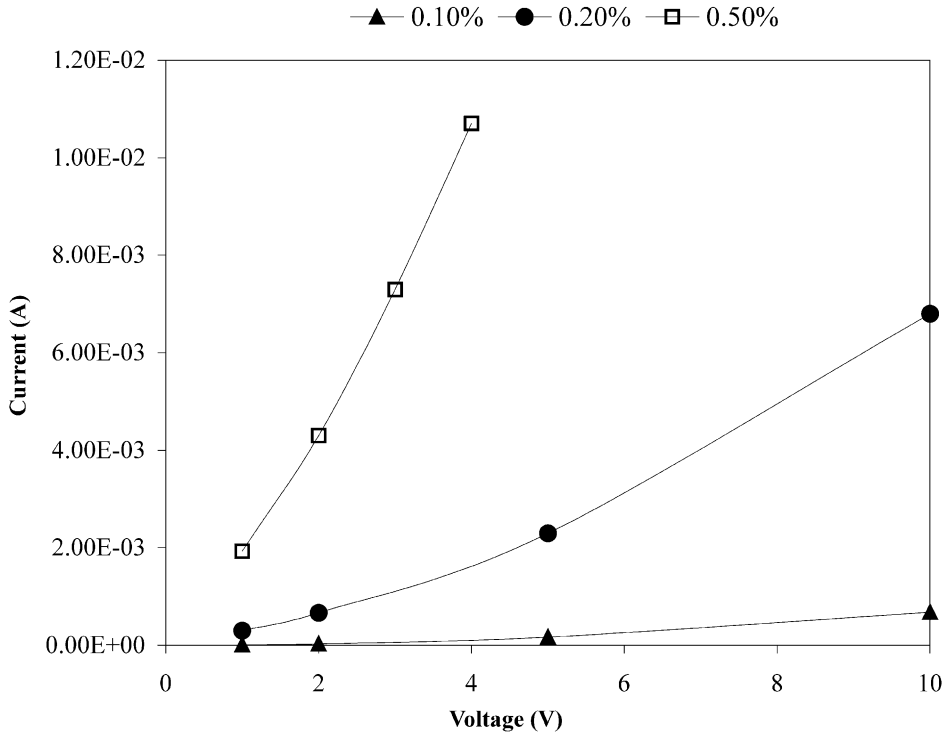

Fig. 3. DC current-voltage behavior of SWNT reinforced polyimide at three different concentrations.

adjacent SWNT, which decreases the effective conductivity of the SWNT [14,15]. The value of A is reduced since the SWNT do not form a network by physical contact. It is reasonable to expect that at much higher SWNT loading, a second threshold would be achieved where the SWNT inclusions contact directly, eliminating the contact resistance. In that case, A would approach the conductivity of the SWNT.

The DC surface conductivity showed a similar behavior to the DC volume conductivity, with an overall lower conductivity (Fig. 4). The percolation threshold is higher in the surface measurement than the volume measurement. It is possible that a skin-layer effect may exist where a preferential alignment of the SWNT on the surface reduces the probability of inter-SWNT contact, thus increasing the value of the critical volume concentration. Additional experiments are needed to confirm this conjecture.

3.3. AC electrical measurements

Fig. 5 shows the AC conductivity as a function of SWNT concentration. The AC results confirm the percolation behavior. At concentration levels below the percolation threshold, a strong frequency dependence of the conductivity is observed, but as the concentration ratio increases, the frequency dependence disappears. The specific admittance was plotted in Fig. 6 as a function of frequency at various SWNT concentrations. At 0 and 0.02 vol.%, the specific admittance increased linearly with the frequency in a logarithmic scale, exhibiting a typical capacitor behavior. At loadings in excess of 0.1 vol.%, the composites exhibited a conductive behavior, where the specific admittance is nearly independent of frequency (in logarithmic scale). This result is in excellent agreement with the findings from the DC conductivity measurements, and further confirms that the critical volume fraction is between 0.02 and 0.1 vol.%.

The effect of temperature on the conductivity is complex since a number of factors affect the behavior of the composite, namely the temperature dependence of the SWNT electrical conductivity, the temperature dependence of the CP2 electrical conductivity, the thermal conductivity of the SWNT, and the thermal conductivity of the CP2. Inspection of Fig. 7 shows that the conductivity of both CP2 and 0.02 vol.% SWNT + CP2 increases slightly with temperature, as may be expected for an insulator. The conductivity of the 0.5 vol.% SWNT + CP2 is fairly constant with temperature, with a slight decrease at 125 and 150 °C. This composition is above the percolation threshold at room temperature. As the temperature increases, it is surmised that the distance between two adjacent SWNT remains stable initially due to a combination of thermal expansion of both the SWNT and the CP2. As the temperature further increases, the average distance between the inclusions increases, resulting in a lowering of the conductivity as the contact resistance increases.

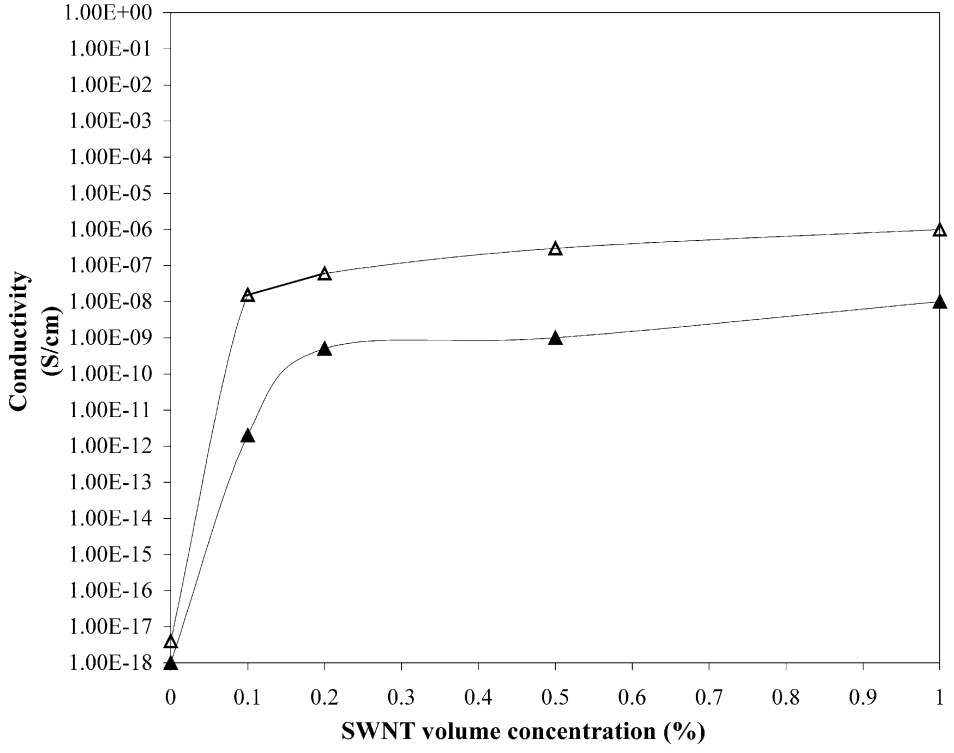

Fig. 4. DC surface and volume conductivity as a function of SWNT volume concentration [open triangle: volume conductivity (S/cm); closed triangle: surface conductivity (S)].

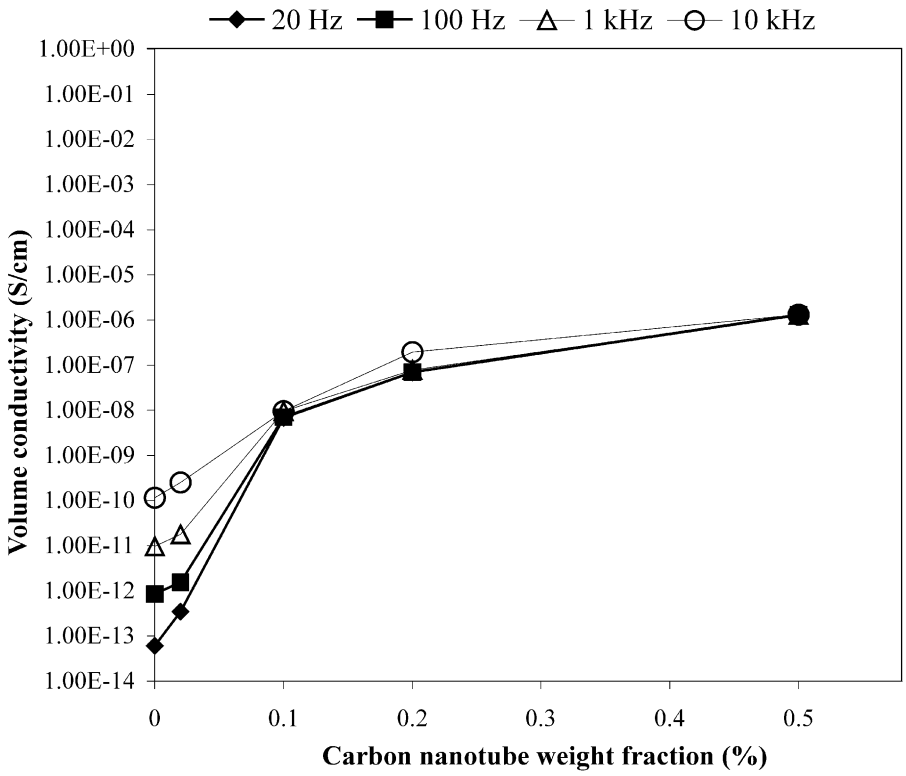

Fig. 5. AC electrical conductivity variations with SWNT volume concentration (measured at 1 V).

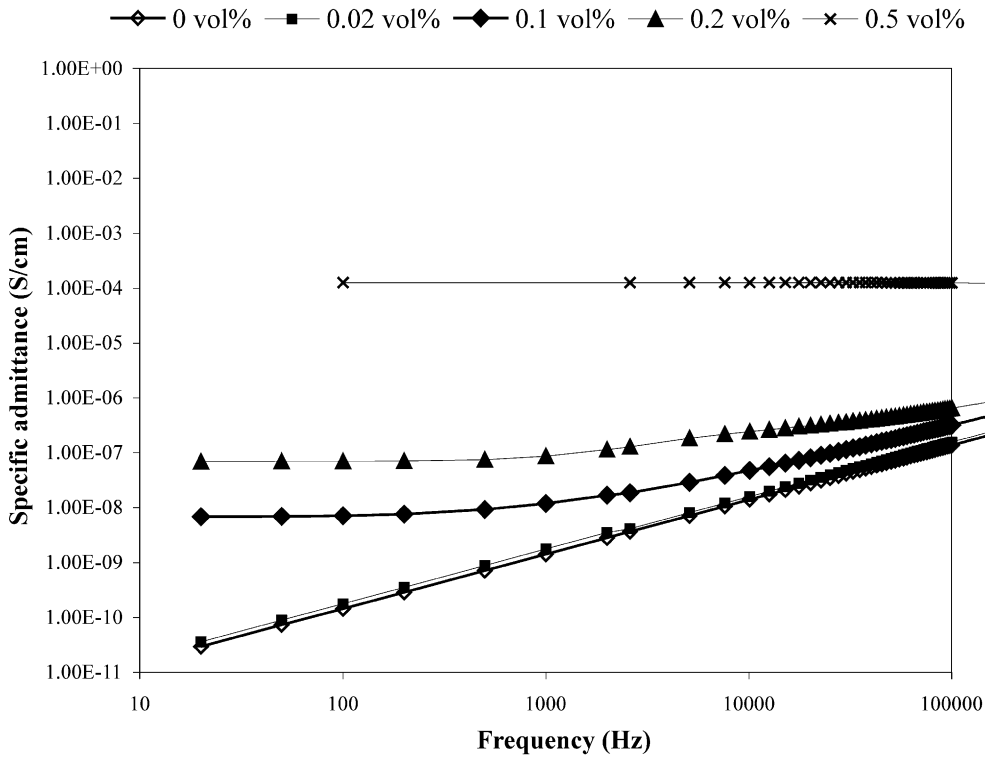

Fig. 6. Specific admittance vs. frequency for 0, 0.02, 0.1, 0.2 and 0.5 vol.% SWNT (measured at 1 V).

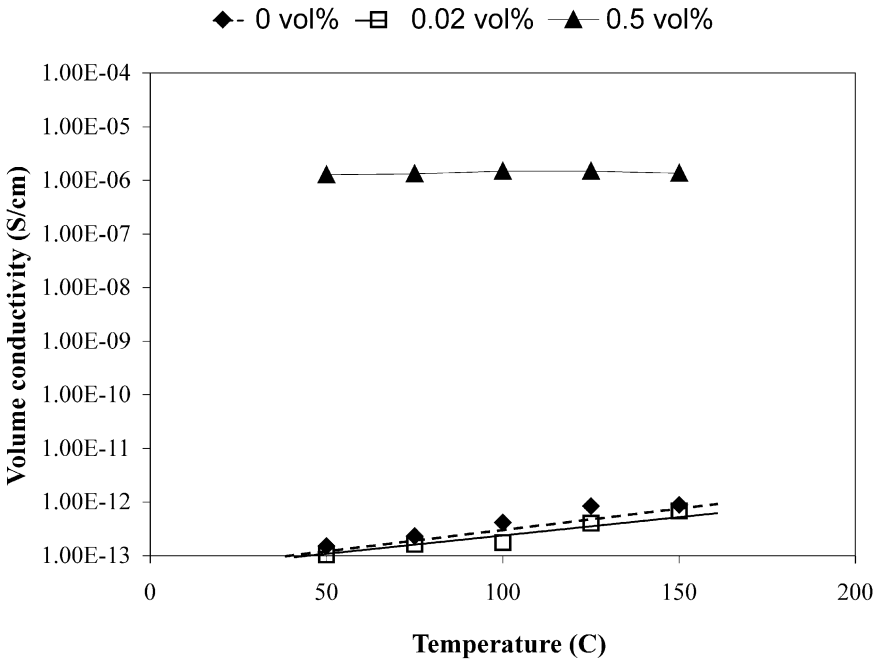

Fig. 7. Temperature behavior of the volume conductivity (at 0, 0.02 and 0.5 vol.%) (measured at 1 V).

4. Modeling and simulation

4.1. Analytical model

Analytical models capable of predicting the percolation threshold of high aspect ratio cylindrical particles embedded in a noninteracting matrix have been developed and applied to microscale particles [16–22]. The applicability of this approach to nanoscale systems is described in this section. The nanotubes are modeled as capped cylinders of radius r and length l, in the limit of very high aspect ratio ($r/l << 1$). The volume of these particles is then:

$$V_{\text{cyl}} = \frac{4}{3}\pi r^3 + \pi l r^2 \tag{4}$$

The excluded volume of an object may be defined as the region of space into which the center of another similar object may not penetrate. For capped cylinders, this volume is expressed as [16–23]:

$$V_{\text{ex}} = \frac{32}{3}\pi r^3 + 8\pi l r^2 + 4\, l^2 r\langle \sin(\gamma)\rangle \tag{5}$$

where the $\langle \sin(\gamma)\rangle$ term describes the degree of alignment of the rods, γ being the angle between two rods. This term ranges from $\frac{\pi}{4}$ for the isotropic samples of interest here to 0 for aligned samples [21]. For isotropic suspensions of capped cylinders, it has been predicted that the percolation threshold (i.e. the critical number density of capped cylinders at percolation) scales as the inverse of the excluded volume [17]:

$$\rho_{\text{c}} \propto (V_{\text{ex}})^{-1} \tag{6}$$

It has further been shown that this proportionality becomes exact in the limit of $r/l \to 0$ [18]. Therefore, the total volume of capped cylinders, at percolation is:

$$V_c = \rho_c V_{\text{cyl}} \tag{7}$$

Dividing Eq. (7) by the total volume of the sample cell yields the volume fraction at percolation:

$$\phi_{\text{c}} = \rho_c V_{\text{cyl}}/V_{\text{tot}} \tag{8}$$

In this expression, V_{tot} is the total volume of the sample, which will be rescaled to 1 in the calculations that follow. The nanotubes used in this work have an approximate radius and length of 0.7 nm and 3 μm, respectively, yielding an aspect ratio ($l/2r$) over 2140. The corresponding r/l ratio is 0.00023, which is sufficiently close to 0 for the percolation threshold approximation given in Eq. (8) to be reliable. The thickness of the films used in the experimental work described above was 45 μm, which is rescaled to 1. After rescaling the length and radius of the cylinders and applying Eqs. (4)–(8) above, the critical volume percentage was predicted to be 0.023%, which is about one half of the experimental value.

As noted in earlier sections, thin SWNT bundles exist in the composites and are uniformely distributed throughout. To evaluate the importance of bundling, the calculation was repeated for a group of seven tubes in a hexagonal arrangement. In this case the effective radius was taken to be 21 Å (2.1 nm), which is the radius of the original tube plus the diameter of one of the flanking tubes (see Fig. 8). This reduces the aspect ratio to about 715 and increases the r/l ratio to 0.0007, which is still close to 0. For this case the volume percentage at

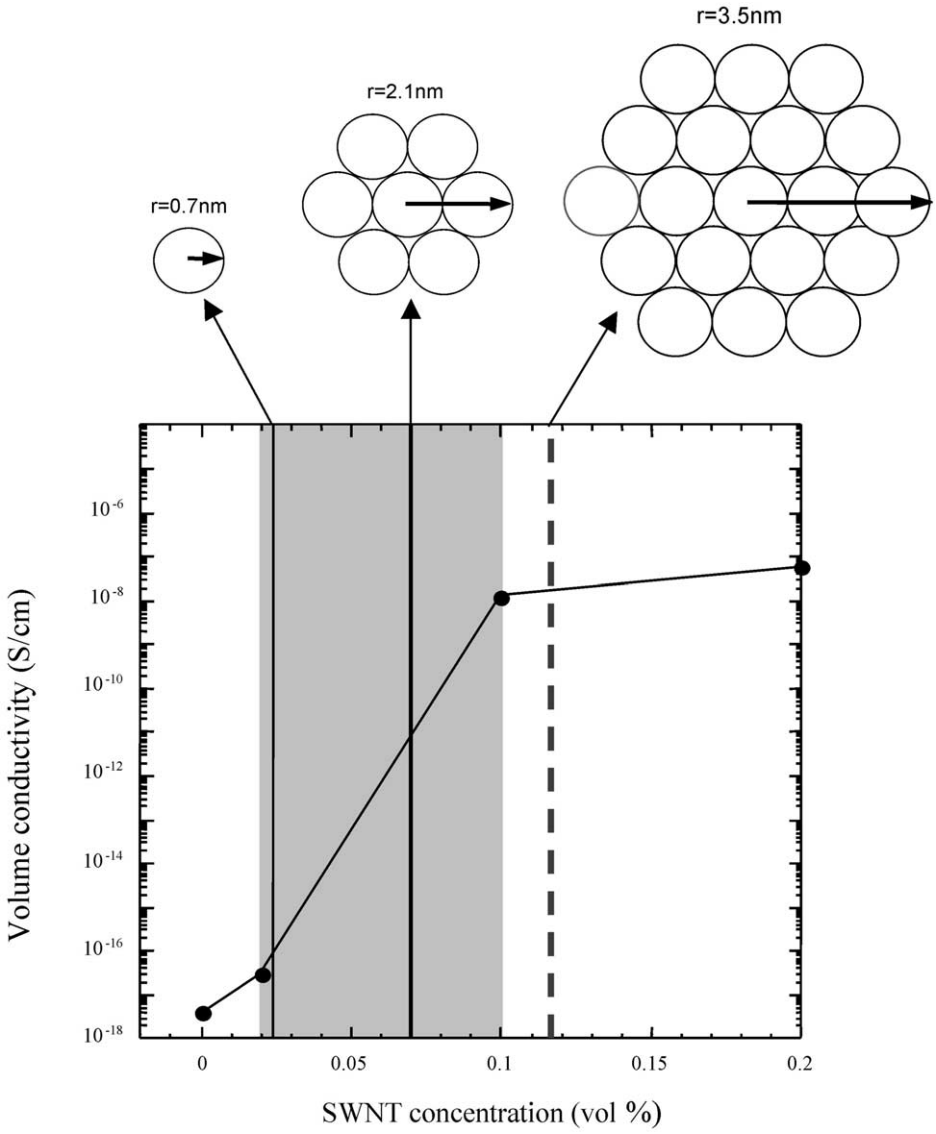

Fig. 8. Comparison between experimental results and analytical predictions in the vicinity of the percolation threshold.

percolation is predicted to be 0.070%, which is in very good agreement with the experiment. Repeating the calculation for a bundle of 19 tubes further increases the critical volume concentration to 0.116%. Fig. 8 illustrates these three cases in the vicinity of the percolation threshold (0 to 0.2 vol.%). The predicted percolation concentrations are shown as solid lines along with the experimental results. It can be seen that the experimental results lie between the single cylinder and seven-cylinder arrangements, indicating that the SWNT are dispersed within the CP2 as very thin bundles made up of a few tubes.

4.2. Numerical simulation

To augment the analytical calculations presented above, numerical simulations have also been performed to determine the critical rod density. As above, the simulation cell size and rod dimensions were rescaled to give a unit volume. The centers of mass of the cylinders were placed randomly within the cell, insuring that no more than half of the cylinder extended beyond the boundary. Orientations were generated by taking the center of mass as the origin a unit sphere and generating a point randomly on the surface, using the method described in [24]. The random unit vector was then rescaled to give the appropriate length for the cylinder. The cluster structures were handled using a modified version of the efficient tree-based union/find algorithm [25]. Two rods were considered touching if the distance of closest approach of their axes was less than $2r$. Newly inserted cylinders were allowed to overlap existing ones, which neglects the hard core repulsion actually found in the real samples. As a result, it was anticipated that the calculated percolation threshold would be overestimated.

Simulations using the model described above were carried out by starting with an empty cell and adding cylinders until a percolating cluster was formed. Percolation was defined as the point at which two opposite walls of the cubic simulation cell were connected by a continuous cluster of cylinders. For any cylinders found to be partially outside of the cell, only the enclosed fraction was considered in the volume fraction calculation. Statistics were collected by performing 1000 independent runs. One representative percolating cell is shown in Fig. 9. Note that the cylinder radii have been artificially enlarged to improve visibility.

The predicted critical volume percentage from these calculations is 0.74%, which is significantly larger than what was predicted by the analytical calculations or found in the experimental study. As mentioned above, one reason for this error is the use of 'soft' cylinders (i.e. no hard core repulsion), which allows regions of space to be occupied by parts of more than one cylinder. This has the effect of increasing the total volume of space considered occupied by particles, while the cell volume remains constant. The net effect is an elevation of the predicted volume percent of cylinders at percolation. Other factors contributing to the error could be the use of an insufficient number of trials to generate the predicted threshold and the constraint that the cylinders are rigidly linear, rather than curved as is observed experimentally. These issues will be treated more fully in a future publication. Nevertheless, the overestimated value (0.74%) predicted by this numerical simulation was still significantly lower than the experimental values reported in the literature [16–18,20].

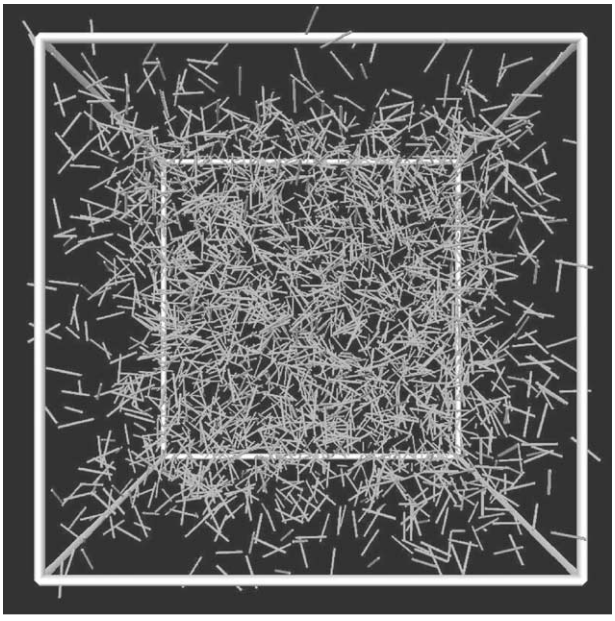

Fig. 9. Numerical simulation of percolation ($\phi c = 0.74\%$).

5. Conclusion

Electrical properties of SWNT reinforced polyimide composites were studied using both DC and AC measurement techniques. The conductivity in these composites results from the formation of conducting paths to the polymer by the SWNT. The measured conductivity could be described by a percolation-like power law equation with a percolation threshold of 0.05 vol.% SWNT. The percolation equation is valid at concentrations above the percolation threshold and only in the vicinity of 0.05 vol.%. Depending on the concentration of SWNT, it is possible to tailor the conductivity of the composite over many orders of magnitude. Agreement between analytical and experimental analysis points to a bundling of SWNT within the matrix.

Acknowledgements

The authors would like to acknowledge Mr. David Callahan, Virginia Commonwealth University, for assistance in gathering some of the conductivity data. This work is supported in part by NASA Grant NCC1-02013.

References

[1] Curan SA, Ajayan PM, Blau WJ, Carroll DL, Coleman JN, Dalton AB, et al. A composite from poly(*m*-phenylenevinylene co-2,5-dioctoxy-*p*-phenylenevinylene) and carbon nanotubes: a novel material for molecular optoelectronics. Adv Mater 1998; 10(14):1091–3.

[2] Coleman JN, Curran S, Dalton AB, Davey AP, McCarthy B, Blau W, et al. Percolation-dominated conductivity in a conjugated-polymer-carbon-nanotube composite. Phys Rev B 1998; 58(12):R7492–7495.

[3] Shaffer MSP, Windle AH. Fabrication and characterization of carbon nanotube/poly(vinylalcohol) composites. Adv Mater 1999;11(11):937–41.

[4] Sandler J, Shaffer MSP, Prasse T, Bauhofer W, Schulte K, Windle AH. Development of a dispersion process for carbon nanotubes in an epoxy matrix and the resulting electric properties. Polymer 1999;40:5967–71.

[5] Kymakis E, Alexandou I, Amaratunga GAJ. Single-walled carbon nanotube-polymer composites: electrical, optical and structural investigation. Syn Met 2002;127:59–62.

[6] Benoit JM, Benoit C, Lefrant S, Bernier P, Chauvet O. Electric transport properties and percolation in carbon nanotube/PMMA composites. Mater Es Soc Symp Proc 2002;706:Z3.28.1–0Z3.28.6.

[7] Park C, Ounaies Z, Watson KA, Crooks RE, Lowther SE, Connell JW, et al. Dispersion of single wall carbon nanotubes by in situ polymerization under sonication. Chem Phys Lett 2002;364: 303.

[8] St. Clair AK, St. Clair TL, Slemp WS. In: Weber W, Gupta M, editors. Proceeding of the 2nd international conference on polyimides. Society of Plastics Engineers; 1987. p. 16–36.

[9] Chesnokov SA, Nalimova VA, Rinzler AG, Smalley RE, Fisher JE. Mechanical energy storage in carbon nanotube springs. Phys Rev Lett 1999;82(2):343–6.

[10] Park C, Crooks RE, Siochi EJ, Evans ND, Kenik EA, Adhesion of polyimide to single wall nanotube bundles revealed by energy filtered transmission electron microscopy. [submitted to NanoLetters.].
[11] Lillehei PT, Park C, Rouse JH, Siochi EJ. Morphology of single wall carbon nanotube-polyimide nanocomposites by scanning probe microscopy. Nano Lett 2002;2:827.
[12] Weber M, Kamal MR. Estimation of the volume resistivity of electrically conductive composites. Polym Comp 1997;18(6):711–25.
[13] Stauffer D. Introduction to the percolation theory. Francis and Taylor; 1991.
[14] Sherman RD, Jacobs SM. Polym Eng Sci 1983;23:36–42.
[15] Liang X, Ling L, Lu C, Liu L. Resistivity of carbon fibers/ABS resin composites. Mater Lett 2000;43:144–7.
[16] Balberg I, Binenbaum N, Wagner N. Percolation thresholds in the three-dimensional sticks system. Phys Rev Lett 1984;52:1465–8.
[17] Balberg I, Anderson CH, Alexander S, Wagner N. Excluded volume and its relation to the onset of percolation. Phys Rev B 1984;30:3933–43.
[18] Bug ALR, Safran SA, Webman I. Continuum percolation of rods. Phys Rev Lett 1985;54:1412–5.
[19] Bug ALR, Safran SA, Webman I. Continuum percolation of permeable objects. Phys Rev B 1986;33:4716–24.
[20] Munson-McGee SH. Estimation of the critical concentration in an anisotropic percolation network. Phys Rev B 1991;43:3331–6.
[21] Celzard A, McRae E, Deleuze C, Dufort M, Furdin G, Mareche JF. Critical concentration in percolating systems containing a high-aspect-ratio filler. Phys Rev B 1996;53:6209–14.
[22] Neda Z, Florian R, Brechet Y. Reconsideration of continuum percolation of isotropically oriented sticks in three dimensions. Phys Rev E 1999;59:3717–9.
[23] Onsager L. The effect of shape on the interaction of colloidal particles. Ann NY Acad Sci 1949;51:627–49.
[24] Marsaglia G. Choosing a point from the surface of a sphere. Ann Math Stat 1972;43:645–6.
[25] Newman MEJ, Ziff RM. Fast Monte Carlo algorithm for site or bond percolation. Phys Rev E 2001;64:016706.